1-1-2006

Learning and Memory in the Cav1.2 Knockout Mouse

Jessica Ann White

LEARNING AND MEMORY IN THE $Ca_V1.2$ KNOCKOUT MOUSE

by

Jessica Ann White

Thesis

Submitted to the Department of Biology

Eastern Michigan University

in partial fulfillment of the requirements

for the degree of

MASTER OF SCIENCE

in

General Biology

Thesis Committee:

James L. VandenBosch, PhD, Chair

Geoffrey G. Murphy, PhD, Project Supervisor

Tamara Greco, PhD, Member

Glenn K. Walker, PhD, Member

November 8, 2006

Ypsilanti, Michigan, USA

DEDICATION

This thesis is dedicated to

Mildred Mabel FunNell

January 24, 1916 – October 9, 2006

ACKNOWLEDGEMENTS

Many thanks go out to all of the members of the Murphy Lab, our post-doctoral fellow, Amy G. Kuo, Medical Scientist Training Program student Brandon McKinney, doctoral candidate John Perkowski, and the many undergraduate students that we've worked with along the way. Each of you have taught many valuable lessons and have often provided very useful bits of insight into the field of science and about life. To Brandon, a special thank-you for sharing your knowledge in science through Immunoblotting and behavior, as well as your mentoring and assistance with writing.

A very special thank-you is due to Geoff Murphy, my project supervisor, employer, mentor, and friend. This graduate degree would not be complete without the many opportunities provided by you in your lab and at the University of Michigan. I will be forever grateful for these opportunities and will value the lessons learned, whether I continue in the academic and science fields or begin a new chapter in my life. These lessons are invaluable.

A thank-you is also owed to Fei Ding for unraveling all for my technical predicaments! Whew! And thank you to my thesis committee at Eastern Michigan University, Committee Chair James VandenBosch and members Tamara Greco and Glenn Walker.

Most importantly, my never-ending support and thanks to my husband, Chelsea, and to our families. To Chelsea, thank you for quietly supporting me in my return to school, for encouraging but not pushing, and for wiping off my knees and sometimes even holding my hand. To my Mom and Dad, thank you for providing all of your love and belief in me, for understanding, and for instilling in me to always put forth my best. To Chip and Jerri, thank

you for sharing your life and educational experiences, for putting things into perspective, and for providing encouragement through our educational difficulties. And finally, to my Grandmother, to whom this thesis is dedicated, for her tenacious yet gentle, loving ways. This surely would have made her even more proud.

ABSTRACT

Of the many signaling pathways found within neurons, calcium signaling is perhaps the most ubiquitous and versatile. Calcium influx through L-type voltage-gated calcium channels (L-VGCCs) is involved in numerous aspects of neuronal function: activation and regulation of gene transcription, synaptic plasticity, and regulation of neuronal excitability are all modulated by calcium. Because many calcium-related subcellular functions are implicated in the formation and storage of long-term memory, this writer investigated the role of an L-VGCC, $Ca_V1.2$, in hippocampus-dependent learning and memory. Utilizing the *Cre/loxP* gene-targeting system, the $Ca_V1.2$ L-VGCC isoform was conditionally deleted in the forebrain of mice. This extensive deletion was confirmed by RT-PCR and Immunoblotting. To test for spatial learning and memory, a series of Morris water maze experiments were performed. Knockout mice showed no deficits in short-term (24-hr) memory trials; however, on a 30-day memory probe, knockout mice performed significantly more poorly than their littermate controls. These results indicate the importance of forebrain-specific $Ca_V1.2$ for long-term spatial memory.

TABLE OF CONTENTS

LIST OF FIGURES

INTRODUCTION

General structural components of the memory-forming region of the brain.

Deep within the temporal lobe of the brain is the hippocampus, a structure found to be important for the formation of memories. In Greek, the term *hippokampos* means seahorse, named by anatomist Giulio Cesare Aranzi (circa 1564) because when cut into coronal sections, its structure resembles the curves of a seahorse.

It was not until the early 1900s that Russian Scientist Vlasimir Bekhterev described the functions of this structure. Prior to Bekhterev's work, the hippocampus was grouped within the limbic system of the brain with other structures that form emotions, such as the neighboring regions of the cortex. Because of Bekhterev's and others' research, the hippocampus is now thought to be important for learning and memory, specifically declarative and spatial memory.

The hippocampus is divided into several named regions: the dentate gyrus, DG, (also known as the hippocampal formation), CA1, CA2, and CA3 (the *Cornu Ammonis*), CA4 (hilus, a part of the DG), and the subiculum, S, also known as the *hippocampal gyrus* or the *subicular complex*.

Inputs to the hippocampal formation come from the nearby structures of the entorhinal cortex via the axons of the perforant pathway that push through the subiculum. From the DG, structures called mossy fibers run to the hippocampus, where they synapse with neurons of CA3. The neurons of CA3 send axons, called *Schaffer collaterals*, to the CA1 area. The CA1 and CA3 regions also receive inputs from the corresponding regions of

the hippocampus in the contralateral hemisphere of the brain through the commissural fibers that cross over through the corpus callosum (Rosenzweig).

The role of neurons within the hippocampus and memory.

The hippocampus is responsible for both declarative (explicit) and nondeclarative (implicit) memory. Declarative memory is a form of memory that one usually refers to when one speaks of memory. Declarative memories are those of conscious thought - accessible bits of facts and information that are acquired through learning. These memories deal with *what* concepts. There are two forms of declarative memory that are very distinct from one another: semantic memory and episodic memory. Semantic memory is generalized memory, such as the knowledge of a word, its meaning, and is not related to the knowledge of when the word was learned. Episodic memory is autobiographical memory that pertains to an individual's particular history or a recollection of a specific time and place (Rosenzweig).

Nondeclarative memory, or procedural memory, is a form of memory shown by performance rather than by conscious recollection (*how* concepts) (Rosenzweig). Skill learning, priming and conditioning are several forms of nondeclarative memory. Skill learning refers to performing a challenging task on repeated trials in one or more sessions. Priming, also called repetition priming, is a change in the processing of a stimulus, usually a word or a picture, as a result of a prior exposure to the same stimulus or related stimuli. Conditioning occurs when a conditioned stimulus (CS), which initially will not elicit a response, is paired with an unconditioned stimulus (US), which automatically elicits an unconditioned response (UR). After repeated pairings of the CS and US, a subject will begin demonstrating new learned responses to the CS, called conditioned responses (CR). Russian

physiologist Ivan Pavlov pioneered the idea of classical conditioning when he used the tone of a bell (the CS) paired with food (the US) to elicit a CR of salivation in dogs.

In general, psychologists and neuroscientists state that the essential role of the hippocampus is the formation of new memories about experienced episodic events. However, some researchers prefer to consider the hippocampus as part of a larger medial temporal lobe memory system that is responsible for general declarative memory.

Structural components of the neuron, neurotransmitters and action potentials.

The nervous system consists of thousands of cells called neurons. Each neuron is composed of a cell body, dendrites, and axons. Most neurons interact through chemical synapses, comprised of pre- and postsynaptic cellular components, in which dendrites and axons abut.

The starting point for activating a synapse is an action potential (AP), a regenerative electrical signal triggered by depolarization (a decrease in polarization or electrical charge), which travels along the axon of the presynaptic cell. When the AP reaches the synapse, voltage gated calcium channels (VGCC) in the presynaptic membrane transiently open. Through a series of poorly defined steps, VGCCs can cause synaptic vesicles to fuse with the cell membrane, releasing neurotransmitters into the synaptic cleft. The synaptic cleft is a narrow space approximately 20 nm wide between the two cells. The released neurotransmitters then diffuse across the cleft and bind to receptors on the postsynaptic membrane (Franks and Sejnowski). Different transmitters can cause either an increase or a decrease in the probability that the postsynaptic cell will regenerate an AP and relay signals to neighboring neuronal structures (Franks and Sejnowski).

Many of the excitatory synapses in the mammalian brain are found on dendritic spines, small protrusions from the shaft of a dendrite, whose primary function may be to compartmentalize Ca^{2+} (Franks and Sejnowski). The increased concentration of Ca^{2+} in the dendritic spines triggers Ca^{2+}-dependent kinases that lead to the induction of long-term potentiation (LTP), a phenomenon that will be discussed further (Kandel, Schwartz, and Jessel).

Synaptic plasticity, long-term potentiation and long-term depression.

Synaptic plasticity is a phenomenon that refers to any long-lasting form of synaptic modification (strengthening or weakening of APs among synapses) that is synapse specific and depends on correlations between pre- and postsynaptic activity (Abbott and Nelson). A persistent increase in synaptic efficacy, either presynaptic activity or postsynaptic depolarization, is referred to as LTP, whereas a decrease in efficacies is known as long-term depression (LTD) (Gerstner).

LTP and LTD are two basic forms of synapse-specific plasticity. Together, they provide the basis for most models of learning and memory (Abbott and Nelson; Chapman et al.; Franks and Sejnowski). In order to induce LTP, a release of presynaptic transmitters and postsynaptic depolarization must occur concurrently. It has been previously demonstrated that extra Ca^{2+} is required to induce LTP, supporting the hypothesis that this process is dependent on intracellular Ca^{2+} (Chapman et al.; Franks and Sejnowski).

The work of Roger Nicoll et al. and Richard Tsien and Franks and Sejnowski (Nicoll, Kauer, and Malenka; Tsien and Malinow; Franks and Sejnowski) indicates that the influx of Ca^{2+} initiates the induction of LTP and persistent enhancement of synaptic transmission by activating two Ca^{2+}-dependent kinases: the Ca^{2+}/Calmodulin kinase (CaM kinase, or CamK)

and protein kinase C (PKC). These enzymes function to catalyze phosphorylation (the addition of phosphate groups to protein molecules), which changes the properties of many proteins. The blocking of these kinases can prevent the induction of LTP (Rosenzweig). CaMK is unique because it remains active once blocked by Ca^{2+}, thus allowing it to assist in the maintenance of LTP.

Calcium influx, synaptic receptors, and their structures.

There are two main sources of Ca^{2+} influx in the neurons of the hippocampus: the ligand-gated channel, N-methyl-D-aspartate (NMDA-type) glutamate receptor, and the VGCC. Neuronal NMDA channels are doubly gated, responding both to voltage and to the binding of glutamate to the receptor complex, making them unique (Kandel, Schwartz, and Jessel). Glutamate is the major excitatory transmitter in the brain and binds to both the NMDA and AMPA ionotropic receptors of the postsynaptic membrane (Franks and Sejnowski). NMDA receptors also control a cation channel of high conductance that is permeable to Ca^{2+} as well as to Na^{+} and K^{+} (Kandel, Schwartz, and Jessel).

The voltage dependence of the NMDA receptor is due to a mechanism that is different from the voltage-gated channels that generate action potentials. Changes in membrane potential are translated into conformational changes in the channel by an intrinsic voltage sensor. In NMDA channels, an extrinsic blocking particle, extracellular Mg^{2+}, binds to a site in the pore of the open channel and acts like a plug, blocking current flow (Kandel, Schwartz, and Jessel). At the resting membrane potential, Mg^{2+} binds tightly to the channel, but when the membrane is depolarized, Mg^{2+} is expelled from the channel, allowing Na^{+} and Ca^{2+} to enter. Thus, maximal current flows through the NMDA-type channel only when two

conditions are met: glutamate is present and the cell is depolarized (Kandel, Schwartz, and Jessel).

In the 1980s, the discovery of selective agonists specific for glutamate receptors allowed researchers to characterize the pharmacology of synaptic transmission in the hippocampus and the neurochemistry of LTP. More specifically, LTP in CA1 requires glutamate receptors that respond to the glutamate agonist N-methyl-D-aspartate (NMDA).

Another characteristic that makes the NMDA receptor unique is that it opens and closes relatively slowly in response to glutamate, contributing to the late phase of the excitatory postsynaptic potential (EPSP) . The late phase of the EPSP is normally small after a single presynaptic action potential because of the Mg^{2+} block. However, when presynaptic neurons fire repeatedly, allowing the EPSPs to summate and depolarize the postsynaptic cell to a greater extent, the NMDA receptor opens to allow a Ca^{2+} influx. Thus, activation of the NMDA receptor leads to an influx of Ca^{2+} and the activation of CaMK. These biochemical reactions are important for triggering signal transduction pathways that contribute to long-lasting modifications in the synapse that are thought to be important in learning and memory (Kandel, Schwartz, and Jessel).

VGCCs can also participate in the induction of LTP in CA1 although their contribution is typically only detectable when strong tetanic stimulation is used (Chapman et al.; Grover, Teyler, and Robbins; Shankar). Tetanic stimulation consists of a high-frequency sequence of individual stimulations of a neuron. Some of the Ca^{2+}-dependent down-stream signaling pathways that are implicated in LTP induction and maintenance can be selectively recruited by either NMDA-receptor-gated or VGCC-activated Ca^{2+} influx.

For example, mice with point mutations that affect the function of calcium-calmodulin-dependent protein kinase II (αCaMKII) show small residual LTP in CA1 that is not sensitive to NMDA antagonists (Chapman et al.; Grover and Teyler). Conversely, Ca^{2+} entering through VGCCs appears to activate protein kinase C (PKC) selectively (Cavus and Teyler; Chapman et al.).

The influx of Ca^{2+} channels have been implemented in various forms of learning and memory (Son and Brinton). Although the exact mechanism is not understood, it seems likely that calcium activates or regulates transcription factors in the nucleus. For example, increases in the concentration of Ca^{2+} triggers phosphorylation and activation of CREB (Silva et al.). cAMP is a responsive element binding protein (CREB) from a large family of structurally related transcription factors that bind to promoter cAMP responsive element (CRE) sites (Silva et al.). This transcription factor is a component of intracellular signaling events that regulate a wide range of biological functions, from spermatogenesis to circadian rhythms and memory.

Evidence from *Aphysia*, *Drosophila*, mice, and rats shows that CREB-dependent transcription is required for the cellular events underlying long-term, but not short-term, memory. Genetic and pharmacological studies in mice and rats demonstrate that CREB is required for a variety of complex forms of memory, including spatial and social learning, thus suggesting that CREB may be a universal modulator of processes required for memory formation (Silva et al.). When phosphorylated, CREB (and CREB family proteins) can modulate the expression of genes with CRE binding sites (Lee and Masson; Chapman et al.).

Calcium channels – their structure, function, and the importance of $Ca_V1.2$.

Ca^{2+}channels couple changes in neuronal activity with rapid changes in intracellular Ca^{2+} levels. Changes in Ca^{2+} levels in turn regulate a diverse range of cellular processes (Lipscombe, Pan, and Gray). These same currents have diverse physiological and pharmacological properties and thus have been given alphabetical names and have also evolved for distinct classes of Ca^{2+} currents (Lipscombe, Pan, and Gray; Ertel et al.).

Of the 5 types of Ca^{2+} channels, the N, P/Q, R, T, and L, the L-type Ca^{2+} channels were the focus of this project. The L-type Ca^{2+} channels require a strong depolarization in the postsynaptic neuron for activation and remain active for long periods of time (Hell et al.; Ertel et al.). Of the ten voltage-gated Ca^{2+} channels, four are responsible for mediating the L-type Ca^{2+}currents: channels $Ca_V1.1$, 1.2, 1.3, and 1.4. $Ca_V1.2$ has been of major interest because of its involvement with learning and memory. The $Ca_V1.2$, or Class C, channels are concentrated in clusters all over the cell body and specifically at the synapses. Platzer (Platzer et al.) and Rajadhyaksha (Rajadhyaksha et al.) both show data supporting that Ca^{2+} influx through neuronal L-type Ca^{2+} channels into the soma modulates gene transcription, thus coupling synaptic excitation to transcriptional events to contribute to neuronal plasticity.

Voltage-gated calcium channels and their structural components.

There are many types of VGCCs, some of which are high-voltage-activated (HVA) or low-voltage-activated (LVA). The T-type channel is the only channel designated as an LVA (Moosmang et al.). The HVA VGCCs are hetero-oligomers with an alpha1 pore-forming subunit (α1), a glycosylated subunit that is mostly extracellular (α2), a small membrane-spanning subunit (δ) that is disulfide-bonded to α2, and a cytoplasmic globular protein (β) (Halling, Aracena-Parks, and Hamilton). Although the functions of these subunits are not clearly understood, they are thought to participate in assembly of VGCCs, docking of other

proteins to VGCCs, movement of the channel to the membrane, and regulation of channel properties (Halling, Aracena-Parks, and Hamilton).

The ion channel pore is formed by a α1 subunit, which has four transmembrane domains, each composed of six transmembrane helices. The activities of several of the HVA-type VGCCs are regulated by Ca^{2+}, a process that requires the Ca^{2+}-binding protein calmodulin (CaM) (Halling, Aracena-Parks, and Hamilton).

L-type Ca^{2+} channels form multisubunit complexes containing different isoforms of pore-forming α-1 subunits, termed α-1C, α-1D, α-1F, and α-1S. L-type Ca^{2+} channels formed by α-1C represent the most abundant isoform in the cardiovascular system. It is therefore believed that the therapeutic effects of Ca^{2+}-antagonist drugs are mainly mediated by blocking of α-1C Ca^{2+} channels (Platzer et al.).

The calcium channels that have been characterized biochemically are complex proteins composed of four or five distinct subunits, each of which is encoded by multiple genes. The α-1 subunit is the largest subunit and incorporates the conduction pore, the voltage sensor and gating apparatus, and the known sites of channel regulation by second messengers, drugs, and toxins (Ertel et al.).

Significance of $Ca_V1.2$ to this project.

The $Ca_V1.2$ channels significant in this project are clustered at synapses of neurons, ideally locating them to contribute to synaptic plasticity. Knockout mice were created for the $Ca_V1.2$ (Seisenberger et al.) isoform; however, the homozygous mutant strain was lethal at embryonic development day 14.5. This is due to the calcium channel pathway's critical role in murine cardiac and smooth muscle development (Seisenberger et al.). Thus, the creation of a conditional knockout was necessary.

MATERIALS AND METHODS

Generating the conditional knockout.

In order to study learning and memory using a viable mouse model with functioning Ca^{2+} channels everywhere except in specific regions of the brain, a conditional knockout mouse was created utilizing the *Cre-loxP* system.

The *Cre-loxP* system is a technique used for the introduction of genetic modifications into specific genes by homologous recombination. Cre recombinase (hereafter referred to as Cre), a 38kDa site-specific bacteriophage P1-derived recombinase protein, is used to mediate the intramolecular and intermolecular site-specific recombination (excision and inactivation of a target gene) between two *loxP* sites. A *loxP* site, the location of crossing over, consists of two 13-base-pair inverted repeats separated by an 8-base-pair asymmetric spacer region (Lakso et al.).

During this technique, one molecule of Cre binds to each inverted repeat, or two Cre molecules line up at one *loxP* site. The recombination occurs in the asymmetric spacer region. The eight bases of the spacer region are responsible for the directionality of the site. The two *loxP* sequences in opposite orientation invert the intervening piece of DNA. Two *loxP* sites in direct orientation ("floxed") determine the excision of the intervening DNA between the two sites, leaving one *loxP* site behind, thus removing the gene of interest. Recombination occurs only in the cells expressing Cre recombinase (Lakso et al.).

The floxed $Ca_V1.2$ mice were generated, using standard recombinant DNA techniques to introduce 2 *loxP* sites inserted into introns 1 and 2, flanking the entirety of exon 2. DNA sequence analysis of correctly targeted clones confirmed the integrity of the *loxP* sites and the presence of the floxed exon in 2 of the clones. Blastocyst injection of these clones

resulted in a single male founder capable of germ-line transmission and was confirmed by Southern blot analysis.

The first $Ca_V1.2$flx mouse was then crossed with a second mouse that contained a *Cre* recombinase transgene under the control of a transcriptional promoter from the α*CaMKII* gene. The alpha isoform of *CaMKII* is expressed postnatally in glutamatergic neurons of the neocortex (Griffith, Lu, and Sun). In offspring that are homozygous for the floxed gene that also carry the *Cre* transgene, the floxed gene will be deleted by *Cre/loxP* recombination but only in those cell types that have an active *Cre* gene promoter (Kandel, Schwartz, and Jessel; Branda and Dymecki). By this means, efficient gene knockout is accomplished in postmitotic glutamatergic neurons in a highly restricted manner, limited primarily to neurons of the cortex and hippocampus (Kandel, Schwartz, and Jessel).

F^2 hybrids were produced and maintained by crossing the two strains $Ca_V1.2$flx ($Ca_V1.2^{f/-}$) and the $Cre1557^+$. Offspring from this cross were used for complete characterization, both biochemically and behaviorally.

Animals.

$Ca_V1.2$flx mice are maintained by breeding the heterozygous ($Ca_V1.2^{f/-}$) animal with a 129/SVE wildtype animal. The $Cre1557^+$ animals are maintained by crossing the Cre-positive transgenic animal with a C57/BL6 wildtype animal. All wildtype animals are purchased from Taconic Farms. In maintaining these lines, the sex of the animals for either the transgenic animal or floxed animal for breeding is not critical. Offspring from the maintained (first) cross are then intercrossed: $Ca_V1.2^{f/-}$ x $Cre1557^+$. Again, at this cross, the sex and genotype of the animal need not correlate. The offspring of this cross will produce multiple combinations of genotypes and sexes. In the next intercross of animals, a female

with the genotype $Ca_V1.2^{f/-}$ x $Cre1557^+$ is crossed with a male of the genotype $Ca_V1.2^{f/-}$ x $Cre1557^-$. It has been found that there is a sperm-line deletion in the offspring of floxed animals crossed with $Cre1557^+$ males; thus, a transgenic female must be used. Because the promoter *CaMKII* is expressed in the testes, males that are heterozygous for the floxed gene and also Cre positive will produce offspring heterozygous null $Ca_V1.2$ (Chen et al.). The offspring from this cross are the F^2 hybrids used in all experiments. In Figure 1, a breeding scheme is laid out diagrammatically.

All animals are housed in clear acrylic, shoebox-sized, micro-isolated static cages (Allentown Caging Equipment) in a specific-pathogen-free (SPF) barrier vivarium. Room temperature is maintained at 72ºC ± 2ºC. Fluorescent lights are used to light the facility and are maintained on a timed cycle, turning on at 0600 hours and shutting off at 2000 hours. Positive pressure of the room is maintained by the building ventilation systems. All care for the animals (feeding, watering, and cage changing) is performed by the university's Unit for Laboratory Animal Medicine (ULAM) when the animals are not undergoing behavioral experimentation.

Animal genotyping.

All animals are genotyped by PCR one week prior to weaning in order to determine which will be used for breeding and experiments. All samples for breeding and experiments are genotyped for both the $Ca_V1.2$ and Cre genes. At 14 days of age, mice are anesthetized with Isoflurane in a dessicator, and a 3-5-mm piece of tail is cut for DNA extraction. At this time each animal is also given an ear punch for identification from its littermates. Tail samples are collected in microcentrifuge tubes, given a tube code and number, and set up for digestion with 100 µl of 1-step tail-digestion buffer (50 mM KCl, 10 mM Tris-HCl, pH 9.0,

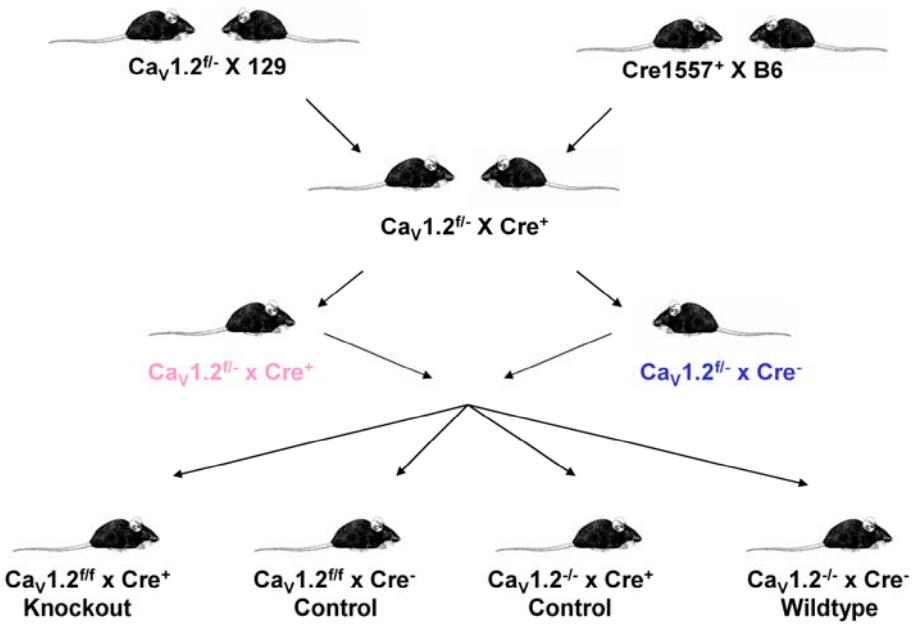

Figure 1. Breeding scheme diagram for maintaining and breeding experimental animals for the $Ca_V1.2$ knockout mouse. $Ca_V1.2$ mice are maintained in the 129/SVE background by crossing heterozygous animals with 129 wildtypes. Cre1557 animals are maintained in the C57/BL6 background by crossing positive transgenic animals with B6 wildtypes. By crossing a $Ca_V1.2^{f/-}$ with a $Cre1557^+$ animal (as shown in the second line, F = founder), offspring from this generation can be crossed to produce the F^1 hybrids. It is important that female animals that are $Ca_V1.2^{f/-}$ x $Cre1557^+$ (f/- Cre+) be crossed with $Ca_V1.2^{f/-}$ x $Cre1557^-$ (f/- Cre-) males, as there is a sperm-line deletion in the male. This final cross of animals produced the F^2 hybrids used for all experiments. Of the six possible genotype permutations, the four above are used for experiments. The true knockout (KO) is indicated by the genotype $Ca_V1.2^{f/f}$ x $Cre1557^+$. The true wildtype (WT) is indicated by the genotype $Ca_V1.2^{-/-}$ x $Cre1557^-$. The two additional genotypes $Ca_V1.2^{f/f}$ x $Cre1557^-$ and $Ca_V1.2^{-/-}$ x $Cre1557^+$ are used to control for the floxing of Exon 2 and for the transgene insertion.

and 0.1% Triton X-100) and 0.75 µl of Proteinase K (0.15mg/ml) per sample. Tail samples are incubated overnight at 56 ºC and then heat inactivated for 10 minutes at 100 ºC before being frozen down at -20 ºC. Once the samples are frozen, they can be thawed and used for genotyping by polymerase chain reaction (PCR.)

Using an Eppendorf MasterTaq Kit, a master mix was made for $Ca_V1.2$ tail samples to be genotyped. A mix was made of the following reagents, per reaction: 8.875 µl of DNase/RNase Free Distilled Water (Gibco), 3 µl of 1.25 µM dNTP (Fisher), 2 µl of 10 X Taq Buffer with 15 mM Mg^{2+}, 1 µl of primer (474/475/476 – 10 µM:10 µM:10 µM – Invitrogen), 0.125 µl of Taq DNA Polymerase, 4 µl of 5 X TaqMaster PCR Enhancer. Once the master mix was made, it was aliquoted into PCR tubes at 19 µl per tube. 2 µl of DNA product from each thawed tail sample was then added to the PCR tube. The sequences for primers 474, 475, and 476 are as follows, respectively: CAT GGA GTC TGG GGG GAG GTC, GTT CCT GCA ATA GCT TGA GGG, and ATA GCA GGC ATG CTG GGG ATG CGG.

Tail samples for Cre were genotyped using BDBiosciences/Clontech taq. A master mix was made with the following reagents: 10.375 µl of DNase/RNase Free Distilled Water (Gibco), 3 µl of 1.25 µM dNTP (Fisher), 2 µl of 10 X Taq Buffer, 1 µl of mutant primer (361/362 – 10 µM:10 µM – Invitrogen), 0.5 µl of wildtype primer (β-actin forward and reverse – 10 µM:10 µM – Invitrogen), 0.125 µl of Taq DNA Polymerase, and 2 µl of Cresol Red for loading dye. Once the master mix was made, it was aliquoted into PCR tubes at 19 µl per tube. 1 µl of DNA product from each thawed tail sample was then added to the PCR tube. The sequences for primers 361/362 and β-actin, forward and reverse respectively, are as follows: 361/362 CAT GTT TAG CTG GCC CAA ATG TTG CTG, CGA CCA TGC

CCA AGA AGA AGA GGA AGG TG, β-actin AGC CAT GTA CGT AGC CAT CC, and CTC TCA GCT GTG GTG GTG AA.

Using a Stratagene Robocycler Gradient 96, samples were run with the following PCR parameters: 1 cycle at 94 ºC for 3 minutes, 30 repeated cycles of 94 ºC for 45 seconds, 62 ºC for 45 seconds, and 72 ºC for 45 seconds, and 1 cycle at 72 ºC for 5 minutes. Samples were held at 6 ºC upon completion of the cycles. After completion of the PCR, all samples were run on a 1.5% agarose gel (Genepure LE agarose and 1 X TAE ((Tris-Acetate-EDTA, pH 8.3)) Buffer from Fisher) using Promega blue/orange 6 X loading dye and 100 base pair (bp) ladder for 70 minutes at 100 volts (power supply: Fisher Scientific FB 300, gel box: Shelton Scientific – IBI QS-710 Quick Screen). Gel imaging was done using a Kodak EDAS 290 imaging system with a UVP, Inc. UV Transilluminator and Kodak 1D v.3.6.5 Scientific Imaging Systems software. Imaging should show that a mutant band is present at ~925 bp and a wildtype band is present at 600 bp.

Molecular Characterization.

RT-PCR (Reverse-Transcriptase Polymerase Chain Reaction).

RNA Isolation.

Each animal was deeply anesthetized, using Isoflurane, and decapitated for brain harvest. Immediately after the brain was harvested, it was placed in a tray of Phosphate Buffered Saline (PBS) on ice and dissected. The cerebellum was removed and placed in a microcentrifuge tube with 200 µl of Trizol (Invitrogen), and the cortex was cut into two hemispheres. Each hemisphere was then peeled back to expose the hippocampus. Cortical and hippocampal segments were dissected and removed and each placed in their own tubes with 200 µl of Trizol. One knockout (KO) and one control animal (f/f Cre-) were used for

this procedure. RNA was isolated from each of the brain regions, using a standard RNA Isolation with Trizol protocol.

Using a pestle and grinder, each brain structure was homogenized until no further chunks were left. An additional 800 µl of Trizol was added to each tube and gently mixed by inverting. All tubes were then incubated at room temperature for 5 minutes. 200 µl of chloroform was then added to each tube, and the tubes were shaken by hand for 15 seconds, followed by a 3-minute incubation at room temperature (RT). Tubes were then centrifuged for 15 minutes at 14,000 rpm in a cold room (4º C). The upper aqueous phase was removed from each tube and transferred to a clean tube. 500 µl of isopropyl alcohol was added to the supernatant of each tube, and the tubes were mixed by gently inverting. Tubes were then incubated at RT for 10 minutes, followed by another centrifugation of 10 minutes at 14,000 rpm at 4 ºC. At this time a gel-like pellet should be seen. The supernatant was removed by vacuum. The pellet was washed once with 500 µl of 70% ethanol at -20 ºC and allowed to air dry for 5-10 minutes. The gel-like RNA pellets were suspended in 25 µl of RNase Free DEPC-treated water (water treated with diethylpyrocarbonate) and incubated at 55 ºC for 10 minutes. The RNA solutions were stored at -20 ºC until quantification.

RNA Quantification.

Hippocampal, cerebellar, and cortical samples were quantified for yield and purity, using the RNA function on a Fisher Scientific accuSeries (accu-622) spectrophotometer. To quantify the samples for yield, 99 µl of DEPC-treated water was added to a cuvette and blanked on the spectrophotometer. 1 µl of RNA was then added to the cuvette, and it was run again on the spectrophotometer. To quantify the samples for purity, 99 µl of Tris-EDTA (TE) was added to a new cuvette and blanked on the spectrophotometer. TE was used for

quantification of purity in order to have a higher ionic strength and pH. This would produce a more reliable absorbance at A_{280} (Sambrook). 1 µl of RNA was then added to the cuvette, and it was run again. Results from the spectrophotometer were given in µg/ml and then converted to µg/µl for further processing.

SuperScript III First-Strand Synthesis System for RT-PCR.

RNA samples were briefly mixed by vortex. Two micrograms of each sample was used to convert total RNA into first-strand cDNA. Using a SuperScript III First-Strand Synthesis System (Invitrogen), 2 µg of total RNA was added to the following reagents of the kit in its own tube: 1 µl of random hexamers (50 ng/µl) and 1 µl of 10mM dNTP mix with DEPC-treated water to 10 µl. Each sample was incubated at 65 ºC for 5 minutes and then placed on ice for at least 1 minute. A cDNA Synthesis Mix was prepared for the above 8 samples by carefully adding the reagents in the following order (all reagents are written per reaction and not totaled): 2 µl of 10 X RT buffer, 4 µl of 25 mM $MgCl_2$, 2 µl of 0.1 M DTT, 1 µl of RNase OUT (40 U/ µl) and 1 µl of SuperScript III RT (200 U/µl). Ten micorliters of the cDNA Synthesis Mix was added to each RNA/primer mixture, mixed gently, and collected by brief centrifugation. Samples were then incubated for 10 minutes at 25 ºC, followed by an incubation at 50 ºC for 50 minutes. All reactions were terminated by incubating the samples for 5 minutes at 85 ºC. Samples were then placed on ice to chill. Brief centrifugation was done to recollect the samples, and 1 µl of RNase H was added to each tube and incubated for 20 minutes at 37 ºC. Samples were then stored at -20 ºC until further use.

PCR.

The double-stranded cDNA product was then created and amplified by PCR. Using an Eppendorf MasterTaq Kit, a master mix was made for the 8 samples. A mix was made of the following reagents, per reaction: 8.875 µl of DNase/RNase Free Distilled Water (Gibco), 3 µl of 1.25 µM dNTP (Fisher), 2 µl of 10 X Taq Buffer with 15 mM Mg^{2+}, 1 µl of primer (Flx RT-PCR1/Flx RT-PCR2 – 10 µM:10 µM – Invitrogen), 0.125 µl of Taq DNA Polymerase, and 4 µl of 5 X TaqMaster PCR Enhancer. Once the master mix was made, it was aliquoted into PCR tubes at 19 µl per tube. One microliter of cDNA product from each sample was then added to the tube. The sequences for RT-PCR primers forward and reverse are as follows, respectively: CGG TGC TAA ATT CTT GGA AGG G and CCA ACC ATT GCG GAG GTA AGC.

Using a Stratagene Robocycler Gradient 96, samples were run with the following PCR parameters: 1 cycle at 94 ºC for 3 minutes, 30 repeated cycles of 94 ºC for 45 seconds, 62 ºC for 45 seconds, and 72 ºC for 45 seconds, and 1 cycle at 72 ºC for 5 minutes. Samples were held at 6 ºC upon completion of the cycles. After completion of the PCR, all samples were run on a 1.5% agarose gel (Genepure LE agarose and 1 X TAE ((Tris-Acetate-EDTA, pH 8.3)) Buffer from Fisher), using Promega blue/orange 6 X loading dye and 100 bp ladder for 70 minutes at 100 volts (power supply: Fisher Scientific FB 300; gel box: Shelton Scientific – IBI QS-710 Quick Screen). Gel imaging was done using a Kodak EDAS 290 imaging system with a UVP, Inc. UV Transilluminator and Kodak 1D v.3.6.5 Scientific Imaging Systems software. Exon 2 deletion will present a band at 578 bp; presence of Exon 2 is represented by a band at 901 bp.

Immunoblotting (Western blotting).

Immunoblotting for brain-$Ca_V1.2$ protein was conducted to determine to what extent the $Ca_V1.2$ subunit was conditionally deleted. For these experiments, $Ca_V1.2^{f/f}$ x $Cre1557^{+}$ (knockouts) and $Ca_V1.2^{-/-}$ x $Cre1557^{-}$ (wildtypes) mice were used. Cortex and hippocampus segments were microdissected in ice-cold PBS. Because channels are susceptible to proteolysis, all procedures were performed at 4 °C. Membrane fractions were isolated by homogenizing in HSE Buffer (10 mM HEPES, 350 mM Sucrose, and 5 mM EDTA, pH = 7.4) containing Complete Protease Inhibitor (Roche Diagnostics, Mannheim Germany). The homogenate was then centrifuged for 5 minutes at 2,000 X g at 4 °C. The supernatant was then removed and centrifuged again at 100,000 X g for 1 hour. The resulting pellet was re-suspended in ice-cold HSE buffer containing protease inhibitors. The protein content of each sample was determined by Bradford assay (Bio-Rad, Hercules, CA), using bovine serum albumin (BSA) as a standard.

Fifty-microgram protein samples from the specified regions were solubilized in Lamelli buffer and applied to a 7.5% Sodium Dodecyl Sulfate – Polyacrylamide Gel Electrophoresis (SDS-PAGE) gel (Bio-Rad, Hercules, CA) for 90 minutes at 200 mA and transferred to Immuno-blot polyvinylidene difluoride (PVDF) membranes (Bio-Rad, Hercules, CA) overnight at 40 mA. Blots were probed with commercial antibodies: anti-human $Ca_V1.2$ (1:200; Alomone Labs, Jerusalem, Israel) and NrCAM (1:40000; Cambridge, UK). Incubation with the primary antibody was followed by washing with PBS-Tween and incubation with the secondary antibody, horseradish peroxidase-conjugated anti-rabbit (1:5000). All blots were washed, and immunoreactive proteins were visualized with an Enhanced Chemiluminescence (ECL) detection system (ECL Plus, Amersham, UK).

Behavioral characterization.

Morris water maze.

The Morris water maze pool is a standard 1.2 meter pool for mice. Water is made opaque with a non-toxic white paint (Van Aken Jazz Liquid Tempera Paint) to hide an escape platform. The plexiglass escape platform is 10 cm in diameter and approximately 1 cm below the water surface. The water line is 15 cm below the rim of the pool. The edge of the pool is 1.5 meters from the nearest visual cue (white walls with each wall's containing a single poster of contrasting color.)

For these experiments, water temperature was maintained at 25 °C ± 2 °C. A camera was fixed to the ceiling directly above the pool at 1.5 meters. The camera was connected to a digital tracking device and processed by a Dell Omniplex 270 computer running Actimetrics Watermaze Software v. 2.6.

Additional mice from the same crosses of F^2 hybrids used for RT-PCR and Western blotting were used in the Morris water maze. To control for the floxing and insertion of the *Cre* transgene, two additional controls were used: $Ca_V1.2^{f/f}$ x Cre^- and $Ca_V1.2^{-/-}$ x Cre^+. Each mouse tested was handled for approximately 2 minutes each day for 7 days prior to the first water maze training trial. On the 8^{th} day of the protocol (day 1 of training), each animal was left on the platform for 15-20 seconds. The mouse was then placed into the water facing the wall of the pool, at 1 of 6 starting locations, and allowed to search for the platform. The animal was allowed 60 seconds to find the platform. A trial ended when the animal either found the platform or spent 60 seconds searching. At the end of each trial, the mouse was allowed to rest on the platform for an additional 15-20 seconds as a reinforcement period.

Animals were given 2 training trials per day for 14 days. The time to reach the platform (latency) was recorded and analyzed by the tracking software.

Probe trials were administered throughout training on the morning following every sixth trial, prior to the start of the two training trials for that day. During the probe trial the platform was removed. The animal was started in a position opposite the training location and allowed to swim for 60 seconds. For analysis, both the amount of time each mouse spent searching in each pool quadrant and the number of times the mouse crossed over the former platform was measured. After the 14th day of training, all mice were allowed to rest for 30 days. On the 51st day of the protocol, all mice were given one more 60-second probe trial (memory test.)

As a control for motivation, swimming ability, and sensory perception, the mice were required to perform in the visible platform version of the water maze the day following the 5th probe trial, or memory test. They were tested on the visible platform test for two trials. A distinct local cue (a blue and yellow block "M" flag) was fixed in the center of the platform. Figure 2 is an image of the layout of the Morris water maze, the starting points around the pool, and the pertaining quadrants during a probe trial. Figure 3 shows a calendar of the training days, including probe trials and memory tests, of the Morris water maze protocol.

Data collected during training and the visible platform test were subjected to a repeated-measures ANOVA with genotype and training days as factors. Probe trials were analyzed comparing the average percentages of time spent in the target quadrant in both groups (unpaired t test) and by making an individual group comparison of the average percentage of time spent in the target quadrant with respect to chance (25%).

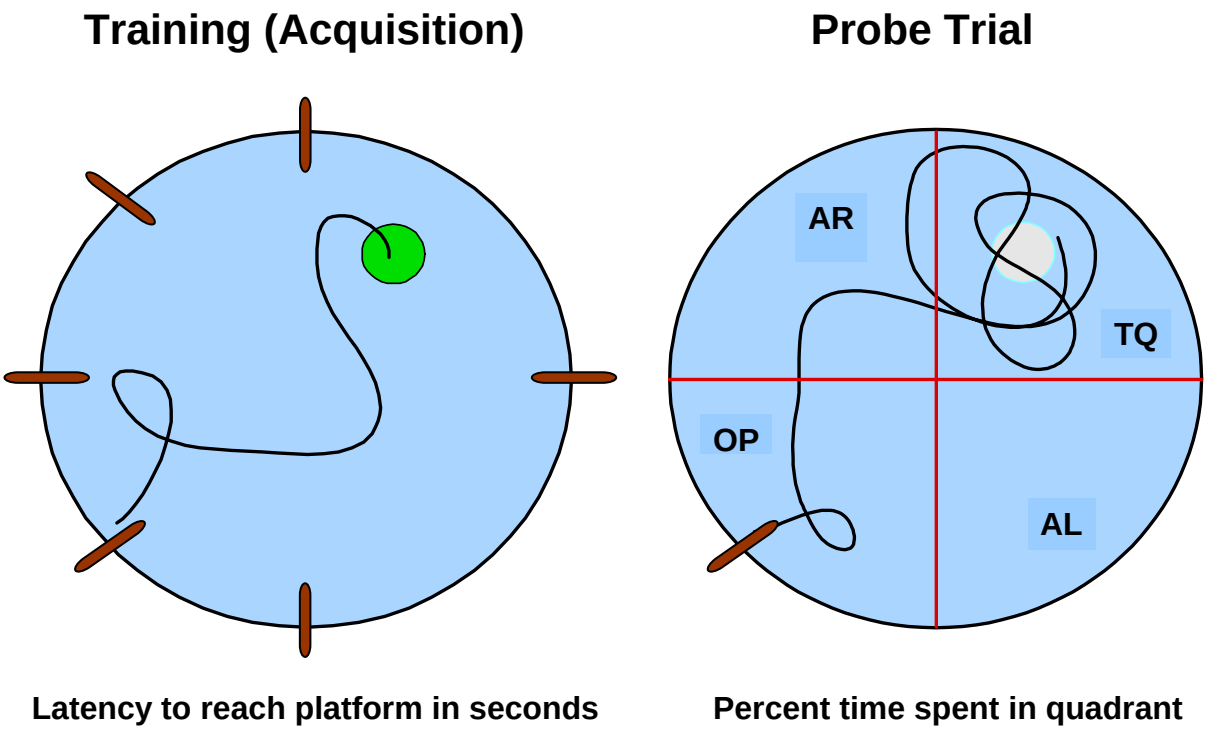

Figure 2. Diagram of the Morris water maze. Training (Acquisition). In the training trial of the Morris water maze, the mouse is placed in the water, facing the wall, at one of the six starting points, indicated by the brown marks. The mouse is allowed to swim for up to 60 seconds or until it finds the platform. The time to reach the platform (latency) is measured in seconds. **Probe Trial.** In the probe trial the mouse is placed in the pool in the quadrant opposite (OP) of the platform, which has been removed. In the probe trial, the time spent in each quadrant and platform crosses is measured. Quadrant TQ is the target quadrant, the area of the pool in which the platform was located. OP is the opposite quadrant of the TQ. AR and AL are the adjacent right and left quadrants of the target quadrant when one is looking down on the pool.

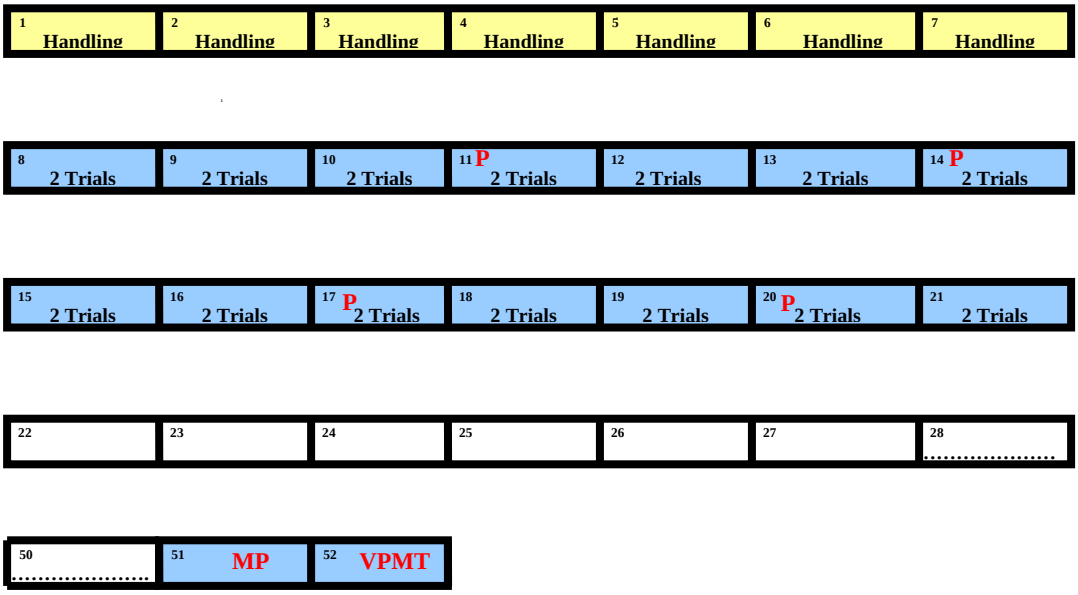

Figure 3. Calendar of the Morris water maze protocol. Days 1-7 indicate days in which mice were handled once a day. Days 8-21 indicate the 14 days of training at two trials per day; a probe trial is indicated by the red P. Starting on day 22 of the protocol, animals were left to rest for three weeks; a memory probe (MP) followed the resting period. The visible platform memory test (VPMT) took place the day following the memory probe.

Massed Morris water maze.

An additional group of mice from the same crosses of F^2 hybrids used for the Morris water maze were used for the Massed protocol of the Morris water maze. In this protocol, only knockouts and homozygous floxed Cre negative animals were used.

Each mouse tested was handled twice a day for approximately 2 minutes each time for 7 days prior to the first day of training. On the 8^{th} day of the protocol, all mice were given 8 trials on the visible platform test. Training trials were administered in blocks of two. A visible platform training trial took place for each animal, in which it was left on the platform for 15-20 seconds. The mouse was then placed into the water facing the wall of the pool, at 1 of 6 starting locations, and allowed to swim to the platform. In this protocol, the platform was rotated to 1 of 4 locations in the pool after every 2 trials. A trial ended when the animal found the platform or spent 60 seconds searching. At the end of each trial, the mouse was allowed to rest on the platform for an additional 15-20 seconds as a reinforcement period. The time to reach the platform (latency) was acquired and analyzed by the tracking software.

Following the visible platform test, on the 9^{th} day of the protocol (training day 2), all animals were exposed to 14 trials of the hidden platform version of the water maze. During these training trials the platform is located in the same position throughout all acquisition trials. All trials were administered in blocks of two. The day following this training, one probe trial was administered to all of the animals by the same means as the trials administered in the spaced Morris water maze protocol. Again, for analysis, both the amount of time each mouse spent searching in each pool quadrant and the number of times each mouse crossed over the former platform was measured. In Figure 4, a calendar of the

Massed version of the Morris water maze shows the number of training days as well as probe trials and memory tests.

Data collected during training and the visible platform test were subjected to a repeated-measures ANOVA with genotype and training days as factors. Probe trials were analyzed comparing the average percentages of time spent in the target quadrant in both groups (unpaired t test) and by making an individual group comparison of the average percentage of time spent in the target quadrant with respect to chance.

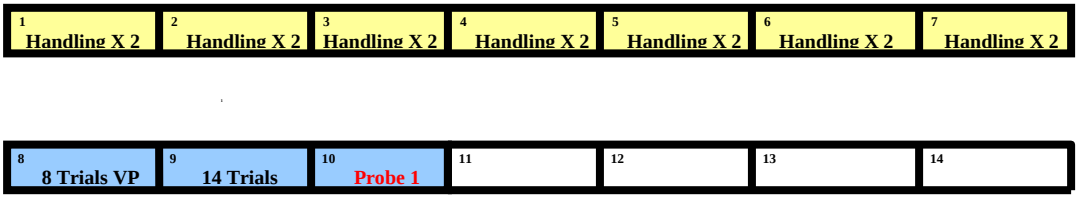

Figure 4. Calendar of training for the Massed Morris water maze protocol. Days 1-7 indicate days in which mice were handled twice a day. On day 8, mice were given 8 trials on the visible platform (VP) from rotating starting points. On day 9, mice were given 14 trials in sets of 2, all from rotating starting points. A single probe trial was given on day 10 in which the platform was removed. Starting on day 11 of the protocol, animals were left to rest for three weeks; a memory probe test (MT) followed the resting period on day 28.

RESULTS

Molecular characterization.

RT-PCR (Reverse-Transcriptase Polymerase Chain Reaction).

RT-PCR, or Reverse Transcriptase Polymerase Chain Reaction, is the process by which DNA is synthesized from messenger RNA (mRNA.) The enzyme reverse transcriptase is a DNA polymerase enzyme that copies single-stranded RNA into double-stranded DNA. This procedure is used to amplify a single strand of RNA by first reverse transcribing it into its DNA complement, followed by amplification of the resulting DNA by PCR. This technique can be used to amplify even the smallest amount of genetic material.

Brain tissue samples harvested from mice of the knockout and control genotype, $Ca_V1.2^{f/f}$ x $Cre1557^{-}$, were used to isolate RNA from the cortex, cerebellum, and hippocampus. Dissected tissue samples were homogenated, and RNA was isolated from the tissue and converted to cDNA (complementary DNA). The cDNA samples were then amplified using standard PCR parameters, with primers designed to amplify sequences flanking Exons 1 and 2.

As shown in Figure 5, the presence of Exon 2 is indicated by a band at approximately 901 bp and is observed in the cerebellum, hippocampus, and both hemispheres of the cortex in the control mouse tissue samples. The deletion of Exon 2 is indicated by a band at approximately 578 bp and can be noted in the hippocampal and cortical samples of the knockout mouse tissue samples. PCR also detected a slight deletion of Exon 2 in the cerebellum of the knockout but not a complete deletion in the cortex and hippocampus, indicated by weak bands at 901 bp. This is likely due to the presence of calcium channels in regions of the cortex not under the *CaMKII* promoter.

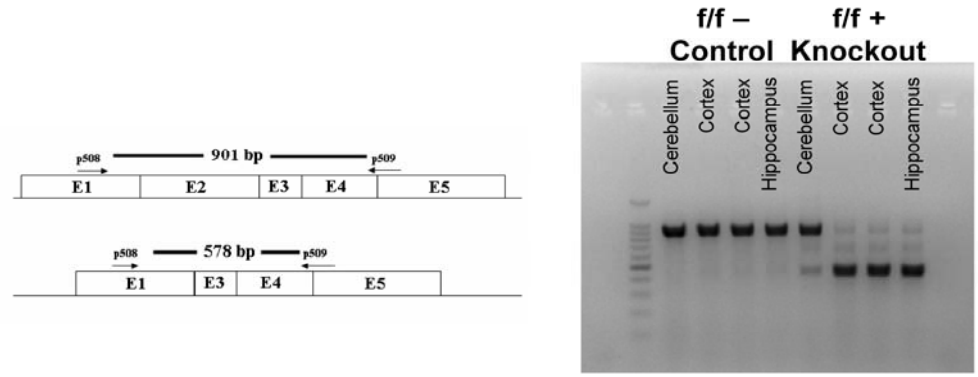

Figure 5. RT-PCR gel image of the $Ca_V1.2$ knockout mouse and control mouse (f/f Cre$^-$). The drawing to the left indicates the construct of Exon 2 and its deletion. The presence of Exon 2 is indicated by the band on the gel image to the right at 901 base pairs (bp). The deletion of Exon 2 can be noted by the band at 578 bp. In the f/f Cre$^-$ control animal there is the presence of the band at 901 bp, indicating that there is no deletion of Exon 2 in the cerebellum, cortex, and hippocampus. In the knockout animal (f/f Cre$^+$) there is a weak band at 901bp in the cortex and hippocampus, and there are strong 901 bp and weak 578 bp bands in the cerebellum, indicating the deletion of the alpha1C channel in the hippocampus and cortex, and partial deletion in the cerebellum. There are two cortex samples per mouse for each hemisphere, left and right.

Immunoblotting (Western blotting).

Immunoblotting is a method of detecting selected proteins in homogenated or extracted tissue samples. This procedure uses gel electrophoresis to separate denatured proteins by mass. Denatured proteins are then transferred from the gel onto a nitrocellulose membrane, where they are probed with antibodies against the protein of interest. The overall procedure signifies the amount of protein within given cells or cellular structures.

As indicated in Figure 6, the results for Immunoblotting reveal that after using antibodies against $Ca_V1.2$ and NrCAM, deletion of the $Ca_V1.2$ protein is noted in the hippocampus and cortex of the knockout animal, indicated by the deletion of a band at approximately 190 kD. The presence of a band at 190 kD in the wildtype animal supports this finding.

Behavioral characterization.

Morris water maze.

The Morris water maze was designed by Richard G. Morris in 1984. It is used to determine to what extent the hippocampus plays a role in spatial learning. In this water maze protocol, 29 animals of the F^2 hybrid cross were tested. Three control animals were dropped from the experiment, leaving 26 for the data analysis. The three animals dropped were cage and littermates, and there were two males housed with a female, an error that had been made during sexing at weaning. Subsequently, during the water maze training trials it was noted that the female's belly had begun to enlarge. Several days later pups were born. The remaining animals used included the following genotypes: eight $Ca_V1.2^{f/f}$ x Cre^+ (KO), six $Ca_V1.2^{-/-}$ x Cre^- (WT), five $CaV1.2^{f/f}$ x Cre^-, and seven $CaV1.2^{-/-}$ x Cre^+ (Controls). For data analysis, true wildtypes and additional controls were consolidated and compared to the KO.

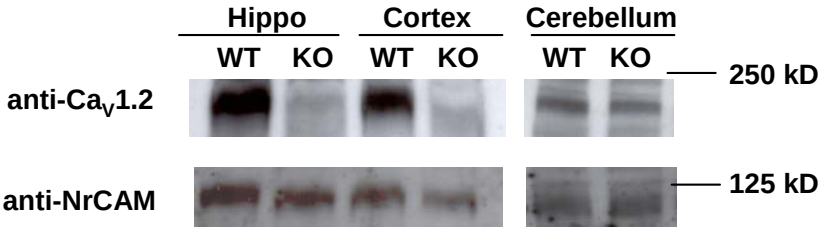

Figure 6. Immunolotting image for $Ca_V1.2$. Antibodies designed against $Ca_V1.2$ were used initially, and membranes were then stripped and reprobed with anti-NrCAM, a ubiquitously expressed neuronal cell-adhesion molecule. A presence of the protein at 190kD can be noted in the wildtype ($Ca_V1.2^{-/-}$ x $Cre1557^{-}$) hippocampus, cortex, and cerebellum. Deletion of $Ca_V1.2$ protein is noted in the hippocampus and cortex of the knockout ($Ca_V1.2^{f/f}$ x $Cre1557^{+}$) sample by the lack of a band at 190kD.

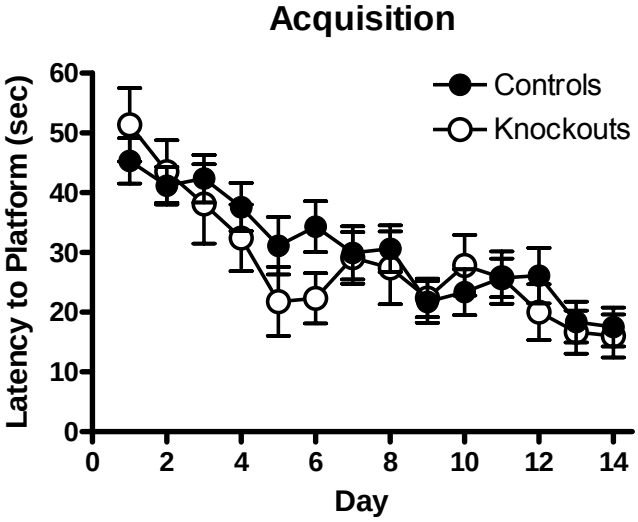

Figure 7. Acquisition of 28 training trials on the Morris water maze. 29 animals of the F^2 hybrid cross were run on the spaced version of the water maze, while 3 were dropped, leaving 26 for analysis. Animals used included the following genotypes: 8 $Ca_V1.2^{f/f}$ x Cre^+ (KO), 6 $Ca_V1.2^{-/-}$ x Cre^- (WT), 5 $Ca_V1.2^{f/f}$ x Cre^-, and 7 $Ca_V1.2^{-/-}$ x Cre^+ (Controls). For data analysis, true wildtypes and additional controls were consolidated and compared to the true KO. Latency (escape) to platform was measured in seconds from the start of the trial. Two training trials were given daily for 14 days. Results from the two training trials each day were averaged. All data are presented as mean ± SEM, showing that $Ca_V1.2$ knockout mice are not impaired on the acquisition phase of the Morris water maze. A repeated-measures ANOVA shows that the latency to platform in both groups decreased as training progressed, with an average escape latency of 16.4 ± 2.5 sec for the controls and 16.0 ± 3.6 sec for the knockouts. The effect of genotype and training on the latency to find the hidden platform is ($F_{(13,312)} = 0.753$; $P = 0.7099$), the effect of genotype on latency is ($F_{(1,24)} = 0.102$; $P = 0.7517$), and the effect of training is ($F_{(1,13)} = 12.774$; $P = < 0.0001$).

Figure 7 plots the 14 days of training (acquisition) for both KOs and controls. All data are presented as mean ± SEM (standard error of the mean.) Latency to platform was measured in seconds from the start of the trial. Two training trials were given daily for 14 days; the average latency of the two trials was plotted for each day. As noted in the figure, the knockouts performed as well as the control animals through the acquisition phase.

Figures 8 and 9 include probes 1 and 4 of the short-term memory probes that were administered during training. Figure 10 includes probe 5, or the long-term memory probe of the protocol, which was administered 30 days after the last training day. Significant difference can be noted in the memory probe in Figure 10 in which the knockout animals perform much more poorly than their control littermates. Figure 11 shows all four short-term memory probes and the long-term memory probe, number 5. The percent time spent in the target quadrant was recorded in seconds for each animal and averaged among the controls and knockouts. Again, all data are shown as mean ± SEM. As noted in the figures, the knockouts performed as well as the control animals during probe trials 1-4. On the long-term memory probe, however, the knockouts showed a significant decrease in the percent time spent in the target quadrant, different from their control and wildtype littermates, demonstrating a remarkable long-term memory impairment.

In a test to measure the ability of animals to locate and climb upon a marked platform, two trials of a visible platform test were administered the day following the last memory test of the water maze protocol. As noted in Figure 12, both the knockout and control animals' latencies to platform were not significantly different (latency averaged less than 10 seconds for all groups.)

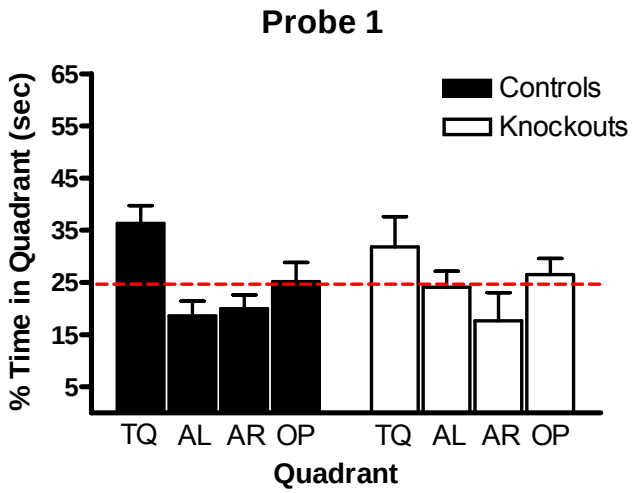

Figure 8. Probe trial 1 of the Morris water maze. Probe 1 of this protocol was administered after day 10 of the protocol, but before the training trials on day 11. In the target quadrant (TQ) where the platform was located, KO animals did not spend a more significant amount of time searching than would be predicted by chance ($t_{(7)} = 1.170$; $P = 0.2804$ single group t test compared with 25%). Control animals did however spend a larger portion of their time selectively searching in the TQ ($t_{(14)} = 3.347$; $P = 0.0048$ single group t test compared with 25%), but the comparison of controls to KOs showed no significant difference ($t_{(21)} = 0.721$; $P = 0.4792$ unpaired t test). All data are shown as mean ± SEM.

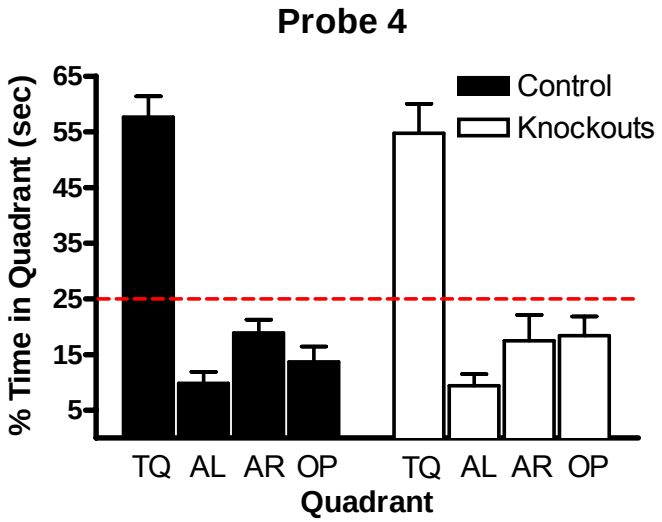

Figure 9. Probe trial 4 of the Morris water maze. Probe 4 of this protocol was administered after day 19 of the protocol but before the training trials on the 20th day. In the target quadrant (TQ), KO animals did spend a majority of their time selectively searching for the area where the platform was previously located ($t_{(7)} = 5.600$; $P = 0.0008$ single group t test compared with 25%). Control animals did also spend a majority of their time selectively searching for the platform in the TQ ($t_{(17)} = 8.712$; $P = < 0.0001$ single group t test compared with 25%). However, there was no significant difference between the control and KO animals in the time spent searching in the TQ ($t_{(24)} = 0.437$; $P = 0.6661$ unpaired t test). All data are shown as mean ± SEM.

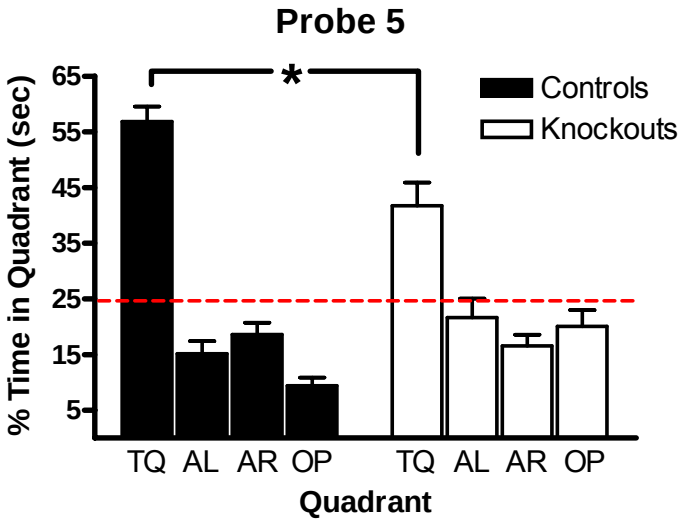

Figure 10. Probe trial 5, or the long-term memory probe, of the Morris water maze protocol. Probe 5 was administered on day 51 of the protocol. In the TQ, KO animals did not spend a majority of their time selectively searching ($t_{(7)} = 3.968$; $P = .0054$ single group t test compared with 25%); however, the control animals did spend a majority of their time selectively searching in the TQ, which showed significance ($t_{(16)} = 11.622$; $P = < 0.0001$ single group t test compared with 25%). Overall there was a significant difference between the KO and control animals in the time spent in the TQ on the memory probe ($t_{(23)} = 3.072$; $P = 0.0054$ unpaired t test) showing a remarkable long-term memory impairment in the KO animals. All data are shown as mean ± SEM.

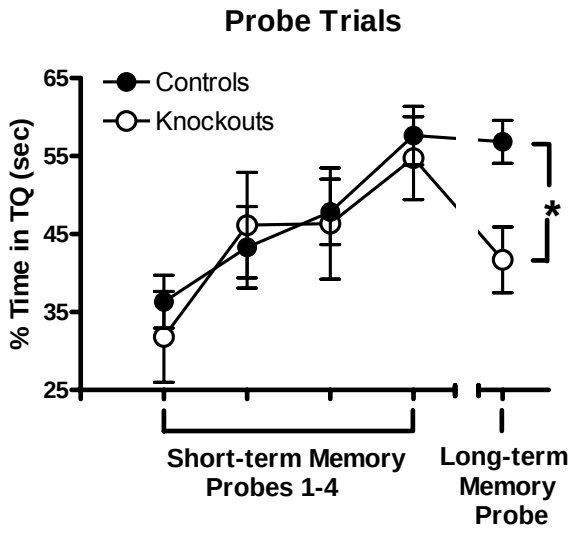

Figure 11. All probe trials of the Morris water maze protocol. Short-term memory probes are indicated as probes 1-4, followed by the long-term memory probe, or probe 5. Significant difference is noted in the long-term memory probe in the time spent searching in the target quadrant between control and knockout mice ($t_{(23)}$ = 3.072; P = 0.0054 unpaired t test). All data are shown as mean ± SEM.

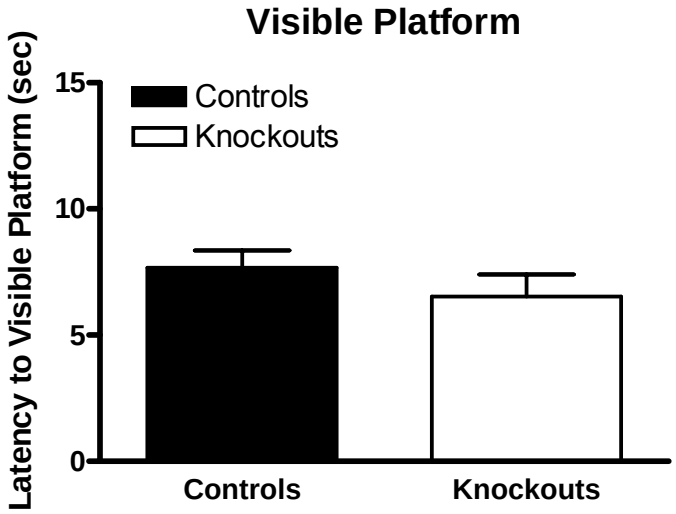

Figure 12. Visible platform test of the Morris water maze protocol. Four trials of the visible platform test were administered on day 52 of the protocol, in blocks of two. All trial times were averaged for control and knockout animals and shown above as mean ± SEM. There is no significant difference between genotypes ($t_{(23)}$ = 0.969; P = 0.3427 unpaired t test).

Massed Morris water maze.

The Massed version of the Morris water maze is a protocol designed to impair spatial memory by administering all acquisition trials over a period of one to two days. In this water maze protocol, 13 animals, seven knockout ($CaV1.2^{f/f}$ x Cre^{+}) and six control animals ($CaV1.2^{f/f}$ x Cre^{-}) of the F^2 hybrid cross were tested. On the first day of the protocol, 8 trials on the visible platform test were administered in blocks of two. In Figure 16, the latency to platform is shown for all eight trials, and each block of two trials is averaged. The knockouts performed as well as their control littermates in all eight visible platform test trials.

On the second day of the protocol, animals were tested over 14 trials, in blocks of two, on the hidden platform version of the water maze. Latency to platform in seconds and trial averages were recorded and plotted in Figure 13. The knockout animals performed as well as their control littermates through trial 8, after which there was a slight decrease in performance in trials 9 and 10, and where they then maintained a decreased latency to platform throughout the remaining trials.

The day following the Massed day of training, all animals were administered one probe trial for which the platform was removed. The percent time in the target quadrant and the number of platform crossings were both recorded. No significant differences between the knockout and control littermates were detected in either the percent time spent in each quadrant or the number of platform crossings, as shown in Figures 14 and 15.

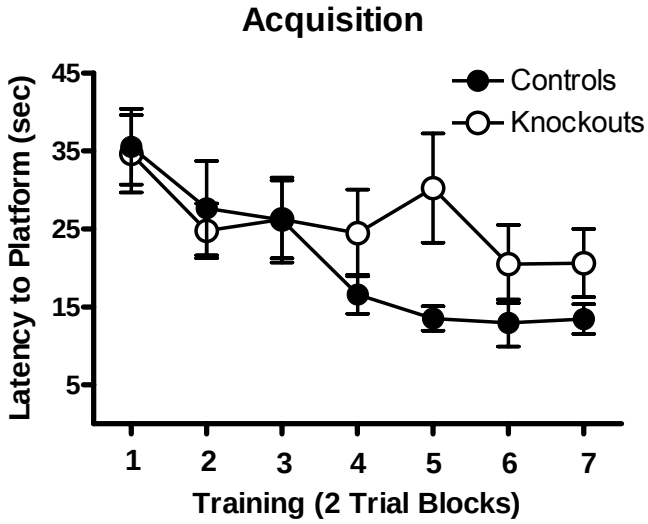

Figure 13. Acquisition of 14 training trials on the Massed protocol of the Morris water maze. Fourteen training trials were run in blocks of two and averaged for data analysis. The latency (escape) to platform was measured in seconds. Thirteen animals were used in this protocol: seven $Ca_V1.2^{f/f}$ x Cre^{+} (KO) and six $Ca_V1.2^{f/f}$ x Cre^{-} (control). All data are shown as mean ± SEM. A repeated-measures ANOVA shows that the latency to platform in both groups decreased as training progressed, with an average escape latency of 13.442 ± 1.912 sec for the controls and 20.621 ± 4.372 sec for the knockouts. The effect of genotype and training on the latency to find the hidden platform is ($F_{(6,66)} = 1.105$; $P = 0.3689$), the effect of genotype on latency is ($F_{(1,11)} = 2.877$; $P = 0.1179$), and the effect on training is ($F_{(1,6)} = 3.9337$; $P = 0.0020$).

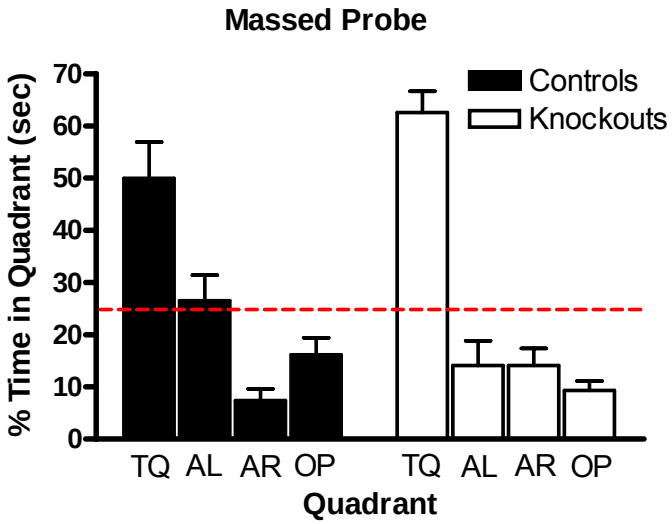

Figure 14. The percent time in each quadrant for probe trial 1 of the Massed protocol of the Morris water maze. One 60-second probe was administered the day following the Massed training, on day 10 of the protocol. In the target quadrant (TQ) where the platform was located, KO animals did spend a more significant amount of time searching than would be predicted by chance ($t_{(6)} = 9.206$; $P = < 0.0001$ single group t test compared with 25%). Control animals also spent a greater portion of their time selectively searching in the TQ ($t_{(5)} = 3.586$; $P = 0.0158$ single group t test compared with 25%), but the comparison of controls to KOs showed no significant difference ($t_{(11)} = 1.169$; $P = 0.1337$ unpaired t test). All data are shown as mean ± mean.

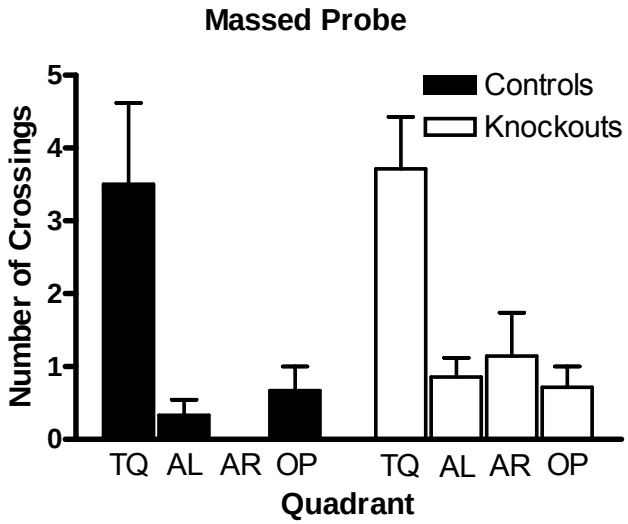

Figure 15. The number of platform crossings in probe 1 of the Massed protocol of the Morris water maze. The number of times the mice swam over the region of the pool in which the platform was once located in the target quadrant (TQ) was recorded and analyzed as ($t_{(11)} = 1.166$; $P = 0.8709$ unpaired t test). The data above are from the same probe trial, also shown in Figure 14, administered on day 10 of the protocol and is presented as mean ± SEM.

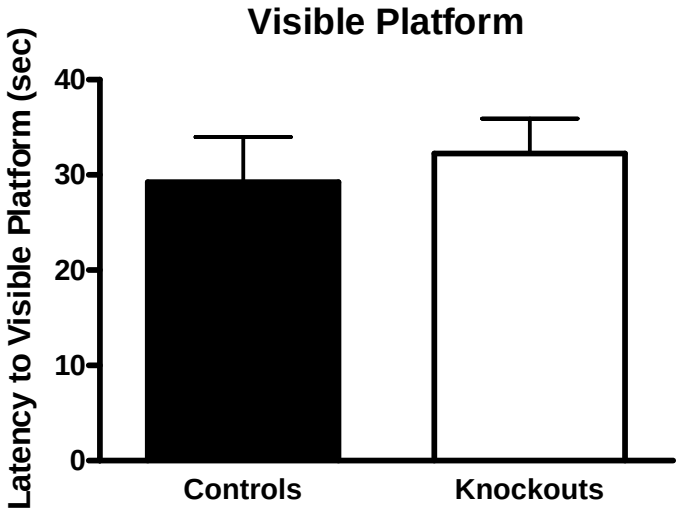

Figure 16. Trial averages for eight training trials on the visible platform of the Massed protocol of the Morris water maze. Eight trials on the visible platform were performed on the same day, in blocks of two, and averaged for data analysis. Latency (escape) to platform was measured in seconds, and block trials were averaged for all knockouts and compared to the block trial averages of the controls. All data are shown as mean ± SEM. A repeated-measures ANOVA shows that the latency to platform in both groups decreased as training progressed, with an average escape latency of 14.025 ± 2.544 sec for the controls and 20.236 ± 4.631 sec for the knockouts. The effect of genotype and training on the latency to find the hidden platform is ($F_{(3,33)} = 0.798$; $P = 0.5036$), the effect of genotype on latency is ($F_{(1,11)} = 0.259$; $P = 0.6207$), and the effect on training is ($F_{(1,6)} = 9.183$; $P = 0.0001$).

DISCUSSION

The goal of this project was to determine the role of the L-type calcium channel, $Ca_V1.2$, in learning and memory. To accomplish this goal, we created a conditional knockout in which $Ca_V1.2$ was deleted in the cortex and hippocampus. I confirmed that $Ca_V1.2$ was deleted in a restricted manner, using RT-PCR and immunoblotting. Using these KO mice, I determined that the deletion of $Ca_V1.2$ results in profound deficits in long-term memory but not short-term memory. As shown in the results, KO mice perform as well as their control and wildtype littermates in the spaced protocol of the water maze and show no deficits in learning after 24 hours (see probes 1-4). However, after a 30-day period of rest, KO mice show a profound deficit in learning and memory (see probe 5).

These results are consistent with the hypothesis that Ca^{2+} signaling plays a critical role in long-term memory (Bito, Deisseroth, and Tsien). How exactly does Ca^{2+} regulate LTM through L-type VGCCs? There is significant experimental evidence that activity-dependent changes in neuronal structure and synaptic remodeling depend critically on protein synthesis. L-type VGCCs are able to respond quickly to millisecond-scale electrical events by generating Ca^{2+} signals, which are known to activate multiple signaling events within the nucleus. Perhaps the best studied of these is the calcium-mediated activation of cyclic AMP response element binding protein (CREB). CREB has been implicated in the storage of long-term memory in numerous species, including *Aplysia* and *Drosophila* as well as rodents (West et al.). Previous studies have shown that knockout mice lacking both the α and Δ isoforms of CREB proteins ($CREB^{\alpha\Delta}$ KO mice) have deficient long-term, but not short-term, memory (Bourtchuladze et al.). Taken collectively, my results suggest that CREB is a likely target for the disrupted Ca^{2+} signaling in the $Ca_V1.2$ KO mice.

In addition to the role that CREB may play in long-term memory formation, several studies have previously demonstrated that alterations of CREB function impact the effect of the varying intertrial interval (ITI) during training (Kogan et al.). Data from *Aplysia* and *Drosophila* indicate that limitations in the levels of CREB-mediated transcription may be one of the many reasons why spaced training results in better memory than Massed training (Kogan et al.; Yin et al.; Pinsker et al.). Yin et al. have shown that genetic studies of memory formation in *Drosophila* support the hypothesis that the formation of protein synthesis-dependent long-term memory requires multiple training sessions, similar to the multiple training days in the water maze. They also described that long-term memory is blocked by induced expression of a repressor isoform of CREB and have shown that the enhancement of long-term memory occurs after induced expression of an activator isoform although it is dependent on the phosphorylation of the activator transgene (Yin et al.).

Consistent with these results, the $CREB^{\alpha\Delta}$ KO mice are particularly impaired in training protocols in which the ITI is short (so-called Massed training) when compared to training accomplished with longer ITIs (so-called Spaced training). In both the water maze and social transmission of food preference (STFP) task, the $CREB^{\alpha\Delta}$ KO mice exhibited memory impairments when the ITI was reduced to one minute or less (Kogan et al.).

To determine whether the deletion of $Ca_V1.2$ interacts with varying ITIs, I conducted a series of experiments examining the impact of decreasing ITIs in the water maze. As described in the results section, deletion of $Ca_V1.2$ does not produce a deficit in spatial learning when short ITIs are used.

Our findings in the Massed protocol of the Morris water maze may differ from some of the currently published data for several reasons. For example, our mice may have

performed differently because of their overall behavior. Further investigations may show that these mice have a neurological condition that impairs them from performing as expected on the basis of the molecular and physiological findings already noted. Another explanation for the unexpected performance of these mice may lie in the design of the protocol used. Water maze protocols can vary across species, and there are a number of variables that can affect learning, such as genetic background, the number of trials per day and the intertrial time allotted (Kogan et al.), the technique and consistency of the researcher, and even the amount of lighting in the testing room and the number of animals housed per cage and their sex. It is also likely that the animals used in our Massed protocol of the water maze were slightly over-trained at 14 trials and perhaps should have been given fewer training trials.

Further investigations may also show that the Massed paradigm is further supported by using massed training in different behavioral tasks, such as the eight-arm radial maze or STFP. In addition, future experiments may include the examination of other $Ca_V1.2$ knockout mice by using different *Cre* lines associated with other regions of the brain, for example, those specific to the CA1, or another region of the hippocampus, or perhaps various regions of the cortex. Also of interest is the neurophysiology and synaptic plasticity of this particular knockout and even the further influence of CREB signaling within the hippocampus.

REFERENCES

Abbott, L. F., and S. B. Nelson. "Synaptic Plasticity: Taming the Beast." Nat Neurosci 3 Suppl (2000): 1178-83.

Bito, H., K. Deisseroth, and R. W. Tsien. "Ca2+-Dependent Regulation in Neuronal Gene Expression." Curr Opin Neurobiol 7.3 (1997): 419-29.

Bourtchuladze, R., et al. "Deficient Long-Term Memory in Mice with a Targeted Mutation of the Camp-Responsive Element-Binding Protein." Cell 79.1 (1994): 59-68.

Branda, C. S., and S. M. Dymecki. "Talking About a Revolution: The Impact of Site-Specific Recombinases on Genetic Analyses in Mice." Dev Cell 6.1 (2004): 7-28.

Cavus, I., and T. Teyler. "Two Forms of Long-Term Potentiation in Area Ca1 Activate Different Signal Transduction Cascades." J Neurophysiol 76.5 (1996): 3038-47.

Chapman, P. F., et al. "Synaptic Plasticity in the Amygdala: Comparisons with Hippocampus." Ann N Y Acad Sci 985 (2003): 114-24.

Chen, A. P., et al. "Forebrain-Specific Knockout of B-Raf Kinase Leads to Deficits in Hippocampal Long-Term Potentiation, Learning, and Memory." J Neurosci Res 83.1 (2006): 28-38.

Ertel, E. A., et al. "Nomenclature of Voltage-Gated Calcium Channels." Neuron 25.3 (2000): 533-5.

Franks, K. M., and T. J. Sejnowski. "Complexity of Calcium Signaling in Synaptic Spines." Bioessays 24.12 (2002): 1130-44.

Gerstner, and Kistler. Synaptic Plasticity and Long Term Potentiation. 2002. Webpage. Cambridge University Press. Available: http://diwww.epfl.ch/~gerstner/SPNM/node71.html. 8/18/04 2004.

Griffith, L. C., C. S. Lu, and X. X. Sun. "Camkii, an Enzyme on the Move: Regulation of Temporospatial Localization." Mol Interv 3.7 (2003): 386-403.

Grover, L. M., and T. J. Teyler. "Two Components of Long-Term Potentiation Induced by Different Patterns of Afferent Activation." Nature 347.6292 (1990): 477-9.

Halling, D. B., P. Aracena-Parks, and S. L. Hamilton. "Regulation of Voltage-Gated Ca2+ Channels by Calmodulin." Sci STKE 2005.315 (2005): re15.

Hell, J. W., et al. "Identification and Differential Subcellular Localization of the Neuronal Class C and Class D L-Type Calcium Channel Alpha 1 Subunits." J Cell Biol 123.4 (1993): 949-62.

Kandel, E. R., J. H. Schwartz, and T. M. Jessell. Principles of Neural Science. Ed. Harriet Lebowitz John Butler. Fourth ed. Vol. 1. New York: McGraw-Hill, 2000.

Kogan, J. H., et al. "Spaced Training Induces Normal Long-Term Memory in Creb Mutant Mice." Curr Biol 7.1 (1997): 1-11.

Lakso, M., et al. "Targeted Oncogene Activation by Site-Specific Recombination in Transgenic Mice." Proc Natl Acad Sci U S A 89.14 (1992): 6232-6.

Lee, K. A., and N. Masson. "Transcriptional Regulation by Creb and Its Relatives." Biochim Biophys Acta 1174.3 (1993): 221-33.

Lipscombe, D., J. Q. Pan, and A. C. Gray. "Functional Diversity in Neuronal Voltage-Gated Calcium Channels by Alternative Splicing of Ca(V)Alpha1." Mol Neurobiol 26.1 (2002): 21-44.

Moosmang, S., et al. "Mouse Models to Study L-Type Calcium Channel Function." Pharmacol Ther 106.3 (2005): 347-55.

Nicoll, R. A., J. A. Kauer, and R. C. Malenka. "The Current Excitement in Long-Term Potentiation." Neuron 1.2 (1988): 97-103.

Pinsker, H. M., et al. "Long-Term Sensitization of a Defensive Withdrawal Reflex in Aplysia." Science 182.116 (1973): 1039-42.

Platzer, J., et al. "Congenital Deafness and Sinoatrial Node Dysfunction in Mice Lacking Class D L-Type Ca2+ Channels." Cell 102.1 (2000): 89-97.

Rajadhyaksha, A., et al. "L-Type Ca(2+) Channels Are Essential for Glutamate-Mediated Creb Phosphorylation and C-Fos Gene Expression in Striatal Neurons." J Neurosci 19.15 (1999): 6348-59.

Rosenzweig, M. R., S. M. Breedlove, and A. L. Lieman. Biological Psychology: An Introduction to Behavioral, Cognitive, and Clinical Neuroscience. 3rd ed. Sunderland: Sinauer Associates, Inc, 2002.

Sambrook, J., and D. W. Russel. Molecular Cloning a Laboratory Manual. 3rd ed. Vol. 3. 3 vols. Cold Spring Harbor: Cold Spring Harbor Laboratory Press, 2001.

Seisenberger, C., et al. "Functional Embryonic Cardiomyocytes after Disruption of the L-Type Alpha1c (Cav1.2) Calcium Channel Gene in the Mouse." J Biol Chem 275.50 (2000): 39193-9.

Shankar, S., T. J. Teyler, and N. Robbins. "Aging Differentially Alters Forms of Long-Term Potentiation in Rat Hippocampal Area Ca1." J Neurophysiol 79.1 (1998): 334-41.

Silva, A. J., et al. "Creb and Memory." Annu Rev Neurosci 21 (1998): 127-48.

Son, M. C., and R. D. Brinton. "Regulation and Mechanism of L-Type Calcium Channel Activation Via V1a Vasopressin Receptor Activation in Cultured Cortical Neurons." Neurobiol Learn Mem 76.3 (2001): 388-402.

Tsien, R. W., and R. Malinow. "Long-Term Potentiation: Presynaptic Enhancement Following Postsynaptic Activation of Ca(++)-Dependent Protein Kinases." Cold Spring Harb Symp Quant Biol 55 (1990): 147-59.

West, Anne E., et al. "Calcium Regulation of Neuronal Gene Expression 10.1073/Pnas.191352298." PNAS 98.20 (2001): 11024-31.

Yin, J. C., et al. "Creb as a Memory Modulator: Induced Expression of a Dcreb2 Activator Isoform Enhances Long-Term Memory in Drosophila." Cell 81.1 (1995): 107-15.

APPENDICES

Appendix A: Chemicals

A

Acetic acid	Fisher Scientific, Fair Lawn, NJ
Acetic anhydride, $C_4H_6O_3$	Sigma, St. Louis, MO
Agarose Genepure LE	ISC, Kaysville, UT

B

Benzamadine hydrochloride	Calbiochem, San Diego, CA
Beta-mercaptoethanol (β-ME)	Sigma, St. Louis, MO
Bicinchoninic acid	BioRad, Hercules, CA
Blotto, Non-fat Dry Milk	Santa Cruz, CA
Bovine Serum Albumin (BSA)	Calbiochem, San Diego, CA

C

Calpain Inhibitor I and II	Sigma, St. Louis, MO
Chaps	Sigma, St. Louis, MO
Chloroform	Fisher Scientific, Fair Lawn, NJ

D

DMSO (Methyl sulfoxide)	Fisher Scientific, Fair Lawn, NJ
DNase/RNase Free Distilled Water	Gibco, Grand Island, NY
dNTPs	Fisher Scientific Fair Lawn, NJ

E	
0.5M EDTA	AccuGENE, Cambrex, Rockland, ME
Enhanced Chemiluminescence Kit	ECL Plus, Amersham, UK
Ethidium bromide	ISC, Kaysville, UT
Ethanol 100%	MStores, Ann Arbor, MI
F	
Ficoll 400	Sigma, St. Louis, MO
G	
Glycerol	Roche, Indianapolis, IN
Glycine	Roche, Indianapolis, IN
H	
Heparin Sodium salt from porcine intestinal mucosa	Sigma, St. Louis, MO
Hepes Buffer	Sigma, St. Louis, MO
Hydrochloric acid	Fisher Scientific, Fair Lawn, NJ
I	
Isoflurane	Baxter, Deerfield, IL
Isopentane	Fisher Scientific, Fair Lawn, NJ
Isopropyl alcohol	Fisher Scientific, Fair Lawn, NJ
K	
Kwik-Stop	Arc Laboratories, Atlanta, GA

L	
Ladder 100bp Blue/Orange 6X loading dye	Promega, Madison, WI
M	
Magnesium chloride, $MgCl_2$	Sigma, St, Louis, MO
Methanol	Fisher Scientific, Fair Lawn, NJ
P	
Phenol:Chloroform:Isoamyl Alcohol	Invitrogen, Carlsbad, CA
Potassium chloride, KCl	Fisher Scientific, Fair Lawn, NJ
Potassium phosphate monobasic, KH_2PO_4	Fisher Scientific, Fair Lawn, NJ
Primers	Invitrogen, Carlsbad, CA
Protease Inhibitor Cocktail	Sigma, St. Louis, MO
Proteinase K, Recombinant, PCR Grade	Roche, Indianapolis, IN
PVDF Membranes	BioRad, Hercules, CA
R	
Ribonuclease A from bovine pancreas	Sigma, St. Louis, MO
S	
SDS-PAGE Gels	BioRad, Hercules, CA
Sodium citrate	Fisher Scientific, Fair Lawn, NJ
Sodium Dodecyl Sulfate (SDS)	Invitrogen, Carlsbad, CA
Sodium chloride, NaCl	Amresco, ISC, Kaysville, UT
Sodium phosphate dibasic, Na_2HPO_4	Fisher Scientific

	Fair Lawn, NJ
Sodium phosphate monobasic, NaH_2PO_4	Fisher Scientific, Fair Lawn, NJ
Sucrose, $C_{12}H_{22}O_{11}$	Fisher Scientific, Fair Lawn, NJ
SuperScript III First-Strand Synthesis System	Invitrogen, Carlsbad, CA
T	
TAE 50X Buffer	Fisher Scientific, Fair Lawn, NJ
Taq Polymerase	Clontech/BD Biosciences San Jose, CA MasterTaq Kit Eppendorf-Qiagen Valencia, CA
Tris	Fisher Scientific, Fair Lawn, NJ
Tris base	Fisher Scientific, Fair Lawn, NJ
Tris-HCl	Fisher Scientific, Fair Lawn, NJ
Triton X-100	Merck, VWR, Batavia, IL
Trizol	Invitrogen, Frederick, MD
V	
Van Aken Jazz Liquid Tempera Paint, White, Non-Toxic	Van Aken, Rancho Cucamonga, CA
Y	
Yeast Extract	Fisher Scientific, Fair Lawn, NJ

Appendix B: Antibodies

Anti-human CaV1.2 Antibody	Alomone, Jerusalem, Israel
NrCAM Antibody Neuronal Marker	Abcam, Cambridge, MA

Appendix C: Markers and Dyes

Bromophenol Blue	Sigma, St. Louis, MO

Appendix D: Buffers and Solutions

100mg/ml Benzamadine	Benzamadine	.5g
	Filtered 1X PBS	Bring to 5ml
Blocking Solution	PBS – Tween	40ml
	Non-fat Dry Milk Powder	2g
Homogenization Buffer	HSE	987µl
	Working Calpain Inhibitor Solution (8µg/ml of each inhibitor)	10µl
	Protease Inhibitor Cocktail	2µl
	Benzamidine (.01mg/ml)	1µl
HSE Buffer	1M Hepes Buffer	1ml
	Sucrose	12g
	0.5M EDTA	1ml
	DI water	Bring to 100ml
5X Laemmli Buffer	DI water	5.2ml
	0.5M Tris pH 6.8	2ml
	Glycerol	3.2ml
	10% SDS	3.2ml
	Beta-mercaptoethanol	.8ml
	1% Bromophenol blue	1.6ml
4% Paraformaldehyde (50ml)	Depc treated water, heated	47.5ml
	Paraformaldehyde	2g
	Shake and heat on stir plate at 68º C	
	10N NaOH	50µl

	HCl	40µl
	20X PBS	2.5ml
	Filter with .45µm filter and 50ml syringe	
	Store at 4º C	
10X PBS pH 7.4 *Westerns*	NaH_2PO_4	2.28g
(Phosphate Buffered Saline)	Na_2HPO_4	11.5g
	NaCl	43.84g
	DI water	Bring to 500ml
	pH to 7.4	
7.5mg/ml Proteinase K	Proteinase K	1.25ml
	1M Tris pH 7.5	2.5 µl
	Depc treated DI water	Bring to 1.5ml
	100% sterile Glycerol	1.5ml
	Aliqout into 200µl tubes and store at -20º	
10X Running Buffer pH 8.3	Tris	30.3g
	Glycine	144g
	SDS	10g
	DI water	Bring to 1l
	pH to 8.3	
10% SDS	SDS	25g
	DI water	225ml
Stripping Solution	Beta-mercaptoethanol	141µl
	10% SDS	4ml
	1M Tris HCl pH 6.8	1.25ml
	DI water	14.61ml
Tail Digestion Buffer Phenol (250ml)	1M Tris-HCl pH 8	24ml
	0.5M EDTA	2.4ml
	5M NaCl	9.6ml
	20% SDS	2.4ml
	DI water	199.2ml
Tail Digestion Buffer 1-Step	KCl	1.86g
	Tris-HCL pH 9	1.55g
	Triton X-100	.5ml
	DI water	Bring to 500ml
10X Transfer Buffer	Tris	30.3g
	Glycine	144g
	DI water	Bring to 1l

Transfer Buffer	10 X Transfer Buffer	1 volume
	DI water	8 volume
	Methanol	1 volume
0.5M Tris pH 6.8	Tris base	30.3g
	DI water	Bring to 400ml
	pH to 6.8	
	DI water	Fill to 500ml
Tris-EDTA (TE)	Tris pH 8	2.5ml
	0.5M EDTA	50ml
	DI water	197.5ml
Working Calpain Inhibitor Solution	Calpain Inhibitor I	80µl
	Calpain Inhibitor II	80µl
	Filtered 1X PBS	840µl

Appendix E: Other Materials

Autoclavable Tubs	Fisher Scientific, Fair Lawn, NJ
Autoclave Tape	Fisher Scientific, Fair Lawn, NJ
Bench Pads	MStores, Ann Arbor, MI
BD 60ml Syringe	Fisher Scientific, Fair Lawn, NJ
Chemical Resistant Multipurpose Tray 13.75x10.6	Fisher Scientific, Fair Lawn, NJ
Dessicator	Fisher Scientific, Fair Lawn, NJ
Dissecting Tools (Scissors, Forceps, Scoop)	Fine Science Tools, Foster City, CA
Ear Punch	Braintree Scientific, Braintree, MA
Filtered Pipette Tips (sterile)	ISC, Kaysville, UT

Guaze Squares, 4x4, Sterile	Fisher Scientific, Fair Lawn, NJ
Nalgene Pore Size: 0.45µm, Case 80 Filters	Fisher Scientific, Fair Lawn, NJ
Microcentrifuge Tubes 1.7ml	ISC, Kaysville, UT
PCR Tubes	ISC, Kaysville, UT
Petri Dishes	Fisher Scientific, Fair Lawn, NJ
Pipette Aide	ISC, Kaysville, UT
Posters for Distal Cues	Ulrich's, Ann Arbor, MI
Razor Blades Single-edged Carbon Steel	Fisher Scientific, Fair Lawn, NJ
Serological Pipette Tips (sterile)	ISC, Kaysville, UT
Superglue, Low Viscosity	WPI, Sarasota, FL
Tube Racks and Trays	Fisher Scientific, Fair Lawn, NJ
Wildtype mice	Taconic Farms, Germantown, NY

Appendix F: Technical Equipment

Autoclave	Primus Sterilizer Company, Omaha, NE
Dell Optiplex GX270 Computer (s)	Dell, Round Rock, TX
Denver Instrument Model 215 Benchtop Research-Grade pH Meter	Fisher Scientific, Fair Lawn, NJ
Eppendorf Research Pro Pipettes	Fisher Scientific, Fair Lawn, NJ
Eppendorf BioPhotometer and Thermal Printer	Fisher Scientific,

	Fair Lawn, NJ
Fisher AccuSeries Analytical Balance	Fisher Scientific, Fair Lawn, NJ
FB200, FB300 FisherBiotech Power Supply	Fisher Scientific, Fair Lawn, NJ
Fisher Isotemp Ceramic/Aluminum Top Stirring Hotplates	Fisher Scientific, Fair Lawn, NJ
Fisher Isotemp 125D Digital Dry-Bath Incubator	Fisher Scientific, Fair Lawn, NJ
Fisher Isotemp Mini Incubator	Fisher Scientific, Fair Lawn, NJ
Fisher Isotemp 215 Water Bath	Fisher Scientific, Fair Lawn, NJ
Fisher Mini Centrifuge	Fisher Scientific, Fair Lawn, NJ
Fostec ACE I Fiber Optic Light Source	Schott, Elmsford, NY
Freezers -20º C	Kenmore, Sears, Hoffman Estates, IL Wood's, Ottawa, OH
Freezer -80º C Revco Ultima II	Thermo, Asheville, NC
IBI QS710, MP1015, HR2025 Horizontal Gel Electrophoresis Unit	IBI Shelton Scientific, Shelton, CT
Ice Machine	Scotsman, Gala Source Denver, CO
Kodak EDAS 290 Imaging System with UVP, Inc. Transilluminotor	Kodak, Rochester, NY
Microwave	Kenmore, Sears, Hoffman Estates, IL
Morris Water Maze and Escape Platforms	Richard Griggs and Geoff Murphy, University of Michigan, Ann Arbor, MI

Purelab Plus Water Filter	US Filter, Siemen, New York, NY
Refrigerator	Danby, Findlay, OH
Reliable Scientific Rocker	RPI, Mount Prospect, IL
Robocycler Gradient 96	Stratagene, La Jolla, CA
Single Pan Hot Shaker	Bellco Glass, Vineland, NJ
Stemi SV II Dissecting Scope	Zeiss, Thornwood, NY
SORVALL Pico Microcentrifuge	Fisher Scientific, Fair Lawn, NJ
Vortex Genie 2	Scientific Industries, Bohemia, NY

Appendix G: Software and Databases

Adobe Acrobat 6.0.0	Adobe Systems, San Jose, CA
Adobe Illustrator 9.0.0	Adobe Systems, San Jose, CA
Adobe Photoshop CS	Adobe Systems, San Jose, CA
Endnote 7.0.0	ISI Research Soft, Berkely, CA
Entrez, PubMed http://www.ncbi.nlm.nih.gov/entrez/query.fcgi	
Filemaker Pro 7.0v1	Filemaker, Inc., Santa Clara, CA
Freezeview 2.1	Actimetrics, Wilmette, IL
GraphPad Prism 4.00	GraphPad, San Diego, CA
HOBOWare	Onset Computer Coporation, Bourne, MA
JMP IN 5.1	SAS Institute, Cary, NC

Kodak 1D 3.6.5 Scientific Imaging Software	Kodak, Rochester, NY
Limelight	Actimetrics, Wilmette, IL
Microsoft Office XP Professional	Microsoft Corporation, Redmond, WA
Statview 5.0.1	SAS Institute, Cary, NC
WaterMaze	Actimetrics, Wilmette, IL

Appendix H: IACUC Approval

This project was approved for the use of animals by the University Committee for the Use and Care of Animals (UCUCA) at the University of Michigan under approval number 08768 as of October 14, 2003. The University's Animal Welfare Assurance Number on file with the National Institute of Health's (NIH) Office of Laboratory Animal Welfare (OLAW) is A3114-01.